



## Crack path simulation for cylindrical contact under fretting conditions

R.A. Cardoso, J.A. Araújo, J.L.A. Ferreira, F.C. Castro

*University of Brasília, Brasil*  
rapha\_2213@hotmail.com

**ABSTRACT.** In this work different strategies to estimate crack path for cylindrical contacts under fretting conditions are carried out. The main goal is to propose and to evaluate methodologies not only to estimate the direction of crack initiation but also the subsequent propagation in its earlier stages, where the stress field is multiaxial, non-proportional and decays very fast due to the proximity with the contact interface. Such complex conditions pose a substantial challenge to the modelling of crack path. The numerical simulations are provided by a 2D Finite Element Analysis taking into account interactions between the crack faces. The results show that, under fretting conditions, models based on the critical plane method are not effective to estimate the crack initiation orientation, while models based on a so called “critical direction” applied along a critical distance provide better results. Regarding the subsequent crack propagation orientation, it was possible to see that stress intensity factor based models where one considers an infinitesimal virtual crack emerging from an original pre-existent crack are powerful mechanisms of crack orientation estimation.

**KEYWORDS.** Fretting fatigue; Crack propagation; Critical distances.

### INTRODUCTION

Fretting is the phenomenon that occurs in mechanical couplings subjected to contact loads and small relative tangential displacement due to oscillatory loads. In association with remote fatigue loads, the process well known as fretting fatigue take place. Failure due to fretting fatigue usually is observed in engineering assemblies under vibration, such as riveted or bolted connections, dovetail joints in turbines and overhead conductors among, others.

The fretting problem is characterized by a strong stress concentration in association with wear, which invariably leads to the nucleation of small cracks. Depending on the level of the stress gradient in such cracks they may arrest, since a threshold value at the crack tip be reached [1]. In order to conduct such analysis criteria able to precise the location, direction of initiation and the further crack path are essential. In these aspects many challenges must be faced, since the fretting problem is characterized for high levels of multiaxiality and non-proportionality.

The aim of this work is to estimate the crack path under fretting conditions in cylindrical contacts assessing some already used methodologies and propose a new methodology to estimate the direction of crack propagation in their earlier stages. Experimental data from literature will be used to confront the theory.

### CRACK ORIENTATION MODELING

As extensively shown in the literature, crack initiation and further propagation is usually characterized by two distinct stages, Fig. 1. The Stage I describes the earlier stage of propagation, commonly governed by Mode II while the Stage II is characterized by a Mode I dominated crack. However, according to [2], Stage I may be



divided in two groups: type 1 when crack initiation is mainly influenced by the range of the shear stress  $\Delta\tau$ , and type 2 when the range of normal stress  $\Delta\sigma_n$  governs the process.

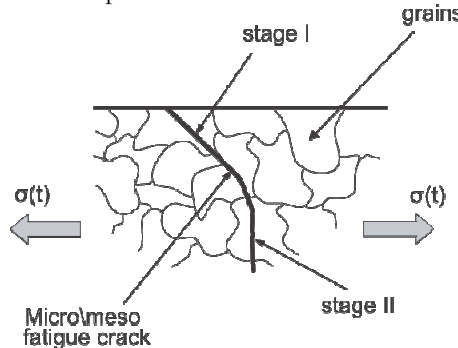


Figure 1: Scheme of classical stages of crack initiation and short crack propagation.

In [3], where tests were conducted in low carbon steel weakened by U-notches to study the high cycle fatigue cracking behaviour, was verified that Stage I, in this kind of stress raiser, is governed by a mixed mode, since the crack profile in Stage I was not parallel to the notch bisector line. It was also noted that the irregular mixed mode dominated path was confined within a distance from the notch tip of the order of  $L$ , the material characteristic length, Eq. (1).

$$L = \frac{1}{\pi} \left( \frac{\Delta K_{th}}{\Delta \sigma_{-1}} \right)^2 \quad (1)$$

where  $\Delta\sigma_{-1}$  is the plain fatigue limit and  $\Delta K_{th}$  is the threshold value of stress intensity factor range, both for a load ratio of -1. Considering these assumptions, two multiaxial criteria based on the theory of critical distances will be applied to estimate the initial crack direction, Fig. 2.

#### *Early stage of crack propagation-The critical direction method combined with the TCD (the critical direction method)*

The theory of critical distances (TCD) [4] can be used in association with any fatigue criterion [5]. So based on the hypothesis that in stage I one may have cracks dominated by the maximum range of normal stress (crack type 2), the crack orientation will be defined here by a line of length  $2L$ , inclined by an angle  $\theta_\sigma$  with respect to the y axis, which maximizes  $\theta$  in Eq. (2), Fig. 2a. Therefore, an important aspect that one should notice in Eq. (2) is that the maximum range of normal stress is always computed perpendicular to the line defined by angle  $\theta$ , i.e., the line  $2L$  (inclined by  $\theta$ ) is discretized in many material points and the maximum normal stress range is calculated for the same plane  $\theta$  for all these points. This procedure provides the critical orientation  $\theta_\sigma$  that a crack of length  $2L$  would have in theory in its stages of initiation and early growth. A similar approach can be used to find the direction that minimizes the shear stress amplitude,  $\Delta\tau$ , Eq. (3). The mechanical basis to support this hypothesis is the fact that, in these planes, less energy is wasted with friction and consequently more energy is available for crack propagation [7].

$$\theta_\sigma = \max_\theta \left( \frac{1}{2L} \int_0^{2L} \Delta\sigma_\theta(r, \theta) dr \right) \quad (2)$$

$$\theta_\tau = \min_\theta \left( \frac{1}{2L} \int_0^{2L} \Delta\tau_{r,\theta}(r, \theta) dr \right) \quad (3)$$

In Eqs. 2 and 3 the integrals are carried out over a constant length  $2L$ , as defined by the so-called Line Method (LM). In a similar way one could assume the point or the area method (for 2D problems) [6], but these will not be assessed here due to space constraints.

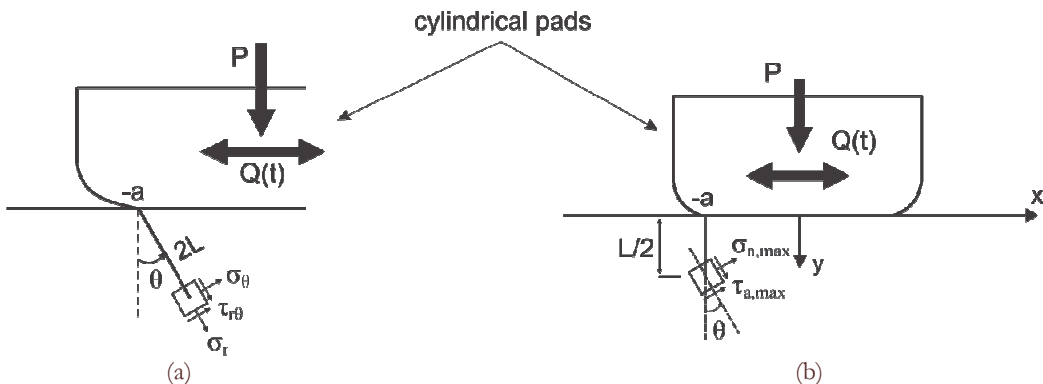


Figure 2: (a) Stress state in the vicinity of the critical zone by means of line method in cylindrical coordinates; (b) critical plane according to the MWCM.

*Early stage of crack propagation-The critical plane method combined with a multiaxial fatigue criterion applied in terms of the TCD (the critical plane method)*

In this case, one assumes that crack initiation is governed by the range of shear stress  $\Delta\tau$  (crack type 1). Considering a critical plane approach, such as the Modified Wöhler Curve Method (MWCM), crack initiation is expected to take place on the material plane that experiences the highest shear stress amplitude. As the shear stress always has the same magnitude in two orthogonal planes, the critical plane between these two planes will be the one with the maximum normal stress along a cycle. Fig. 2b depicts the critical plane method in association with the point method (PM) to estimate the direction of crack propagation. Once again, in order of brevity only the PM will be assessed here.

#### *Crack propagation orientation under fretting conditions*

In fretting, the load conditions are complex and non-proportional, which makes the process to estimate the directions of propagation hard. Now a review of some relevant criteria already used to estimate the direction of crack propagation under fretting conditions will be presented. Notice that all these criteria are valid for pre-existing cracks (stage II).

Classical crack path criteria, such as the maximum tangential stress (MTS) [8], the maximum strain energy density [9] or the maximum energy release rate [10] are not adequate for non-proportional multiaxial loading like in fretting conditions. Taking into account this non-proportionality [2] and [11] considered the following criteria based on [12]:

- (i) Crack propagates in the direction where  $k_1(\theta,t)$  is maximum during a cycle
- (ii) Crack propagates in the direction where  $\Delta k_1(\theta)$  is maximum during a cycle
- (iii) Crack propagates in the direction where  $da/dN(\theta)$  is maximum during a cycle

where  $k_1$  and  $k_2$  are the stress intensity factors in mode I and in mode II, respectively, of an infinitesimally small kinked crack emerging from the pre-existent crack with an angle  $\theta$ , Fig. 3. The expression that relates  $k_1$  and  $k_2$  with the classical mode I and mode II stress intensities  $K_I$  and  $K_{II}$  is given by Eq. (4), where the angular functions  $K_{ij}(\theta)$  are reported in [11] and [13].

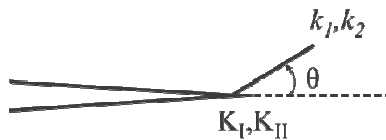


Figure 3: Inclusion of a small virtual crack emerging from the crack tip of a pre-existing crack.

$$\begin{vmatrix} k_1(\theta,t) \\ k_2(\theta,t) \end{vmatrix} = \begin{vmatrix} K_{11}(\theta) & K_{12}(\theta) \\ K_{21}(\theta) & K_{22}(\theta) \end{vmatrix} \begin{vmatrix} K_I(t) \\ K_{II}(t) \end{vmatrix} \quad (4)$$

Based on the MTS criterion, Dubourg and Lamacq [2] proposed that the direction of crack propagation may be found searching for the direction that maximizes  $\Delta\sigma_\theta$  along a cycle, considering that if  $\sigma_\theta < 0$  then  $\sigma_\theta = 0$ , once that compressive stress does not encourage crack propagation. Recently Giner et al. [7], proposed the criterion of the minimum shear stress range, which consists in finding the plane that minimizes the shear stress range at the crack tip, Fig. 4. As the shear stress



always has the same magnitude in two orthogonal planes, the chosen plane for crack propagation direction is the one that experiences the maximum  $\Delta\sigma_n$  (less frictional energy is lost).

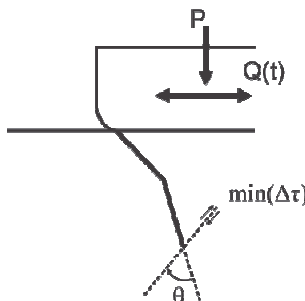


Figure 4: Plane of the minimum shear stress at the crack tip.

## AVAILABLE DATA

To evaluate the accuracy from the aforementioned methodologies experimental data available from tests under fretting conditions will be assessed. All the tests considered are from cylinder-on-plane configuration. Tests were conducted on steel alloy 35NCD16 and AISI 1034 specimens. In both cases the pads were made from different materials, steel 100C6 and chromium 52100 steel, respectively. The mechanical properties are presented on Tab. 1, and the experiments have been reported and discussed in detail in [14] and [15], hence, only essential information necessary to carry out the analyses are briefly presented here.

Material	$E$ (GPa)	$\nu$	$\sigma_Y$ (MPa)	$\sigma_u$ (MPa)	$\sigma_{-1}$ (MPa)	$\tau_{-1}$ (MPa)	$\Delta K_{th}$ (MPa.m $^{1/2}$ )
AISI 1034	200	0.3	350	600	270	-	7
52100	210	0.3	1700	2000	-	-	-
35NCD16	200	0.3	1127	1270	590	460	-
100C6	195	0.3	1500	-	-	-	-

Table 1: Material properties.

The load history applied in the tests are as follows. Firstly, a constant normal load,  $P$ , was applied to the fretting pad and held constant. Then an oscillatory shear force varying between  $\pm Q_a$  was applied. In the tests analysed here there is absence of a bulk load. All the tests were designed to run in partial slip regime, i.e.,  $Q_a/P < f$  where  $f$  is the coefficient of friction in the slip zones. One test will be analysed for AISI 1034 specimen and another for steel alloy 35NCD16. For AISI 1034 the tests analysed presented short crack arrest, hence, this data will be used only to assess the methodologies to estimate crack initiation path. The data from 35NCD16 will be used to assess methodologies in both the initiation and propagation stages. The most important parameters in the load history to carry out the analyses are reported in Tab. 2.

Specimen	$P$ (N/mm)	$Q_a$ (N/mm)	R (mm)	$f$
AISI 1034	227	169	40	0.9
35NCD16	1000	500	80	0.9

Table 2: Parameters of the test; R is the pad radius.

In both test programs after interrupting the experiment the crack path and its extension were observed in an optical microscope by cutting the samples in the centre of the contact zone [16]. In case of AISI 1034 the tests were conducted until  $10^6$  cycles, for 35NCD16 three tests were performed and each of them were interrupted after a different number of cycles and analysed. The crack extension and profile are thus obtained from information collected from different tests.

The results from these tests are reported in Tab. 3 and the crack path is described according to the scheme sketched in Fig. 5.

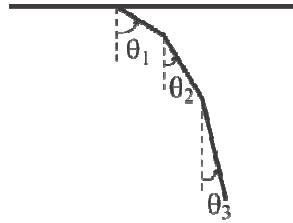


Figure 5: Crack path scheme.

AISI 1034		
1,000,000 cycles	$a_1 = 68 \mu\text{m}$	$\theta_1^* = 30^\circ$
35NCD16		
100,000 cycles	$a_1 = 105 \mu\text{m}$	$\theta_1 = 17^\circ$
250,000 cycles	$a_2 = 130 \mu\text{m}$	$\theta_2 = 13^\circ$
500,000 cycles	$a_3 = 248 \mu\text{m}$	$\theta_3 = 11^\circ$

\* The angle measured by [14] was established through a series of tests, where an angle of  $30^\circ \pm 3$  was observed.

Table 3: Crack path configuration.

## RESULTS FOR CRACK INITIATION ORIENTATION

### Crack initiation direction for AISI 1034

In this case we have a material characteristic length given by  $53.5 \mu\text{m}$ , Eq. (1). The results of the critical direction method are shown in Fig. 6. As can be seen, the estimated angle is very small when the maximum value of  $\Delta\sigma_{n,\text{eff}}$  (only positive values of normal stress are taken into account) is considered, whereas  $\max(\Delta\sigma_n)$  and  $\min(\Delta\tau)$  provide similar results. The range of angles that were investigated were limited to  $-60^\circ$  to  $60^\circ$ , as (i) it doesn't make sense physically to assume crack propagation in directions larger than this (shallow angles practically parallel to the surface) (ii) it reduces the computational cost involved in the calculation when more complicated geometries that requires FEA analysis are assessed.

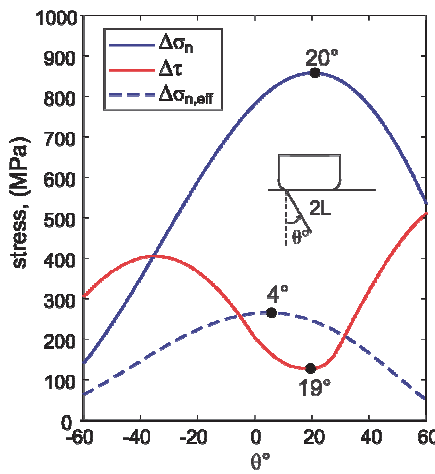


Figure 6: The critical direction method for AISI 1034 data.

Considering the complexity of the stress field and the dispersion involved in the calculation of material parameters as  $L$ , the critical direction criteria based on  $\max(\Delta\sigma_n)$  and  $\min(\Delta\tau)$  provided quite reasonable results in the estimative of the



crack initiation path. However, one should notice that the criterion based on  $\Delta\sigma_n$  is inconsistent, since compressive stresses (usually present during a large portion of the fretting load cycle) do not contribute to crack propagation.

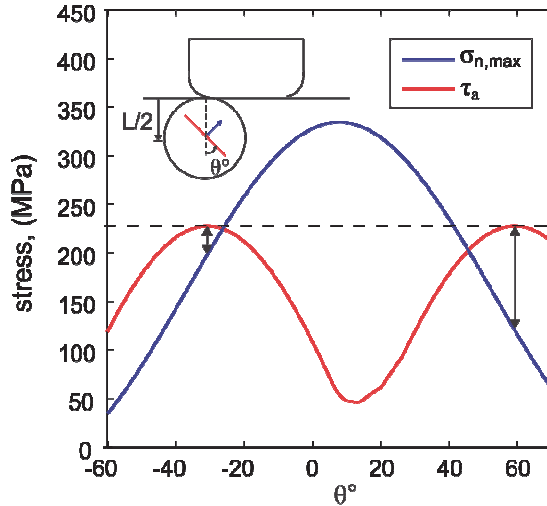


Figure 7: Critical plane model applied in the centre of the process zone ( $L/2$ ) for AISI 1034.

Fig. 7 illustrates the results obtained by the critical plane model applied in the centre of the process zone ( $L/2$ ). Note that the maximum shear stress amplitude is reached in two orthogonal planes ( $-31^\circ$  and  $59^\circ$ ), but the critical plane is the one at  $-31^\circ$  once, between these two planes, it experiences the maximum normal stress during a cycle. Therefore, it is clear that the crack initiation path estimated by this method provides a direction, which is opposite to the actual one ( $30^\circ$ ). Similar kind of inaccuracy to determine crack initiation path from critical plane approach was obtained by Susmel and Taylor [3] for notched components under mixed mode loads.

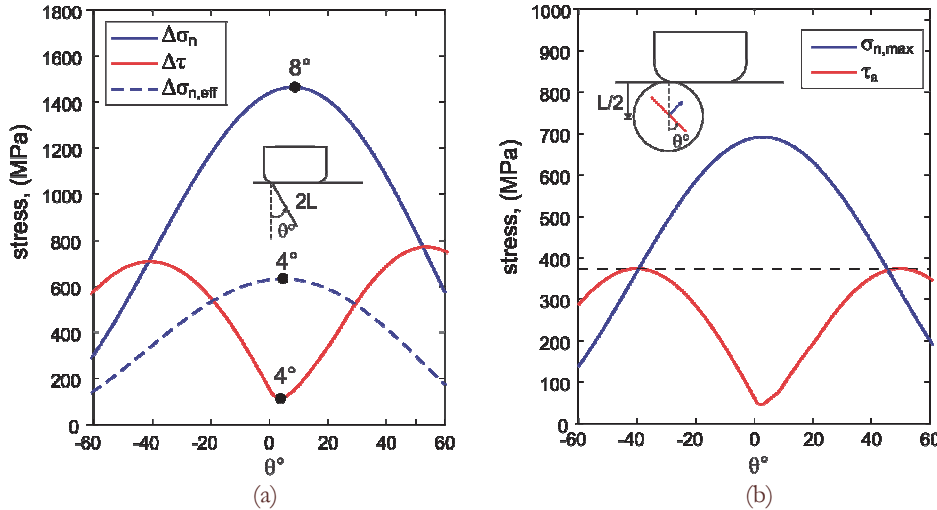


Figure 8: Results for 35NCD16 (a) the critical direction method; (b) the critical plane model applied in the centre of the process zone.

#### *Crack initiation direction for 35NCD16*

Unfortunately, the threshold value for the stress intensity factor range,  $\Delta K_{th}$ , is not available for steel 35NCD16, hence, an estimate based on the work of [17] was done, where the material characteristic length for a steel is given by:

$$L = \left( \frac{36200}{\sigma_u \Delta \sigma_{-1}} \right)^{1.17} \quad (5)$$

where  $L$  is given in mm,  $\Delta\sigma_{-1}$  is the plain fatigue limit (MPa) for a load ratio of -1, and  $\sigma_u$  is the ultimate tensile strength (MPa). The empirical equation has a correlation factor of 0.791, among a wide range of materials data for steels and cast irons. The results for the critical direction method and the critical plane model for the 35NCD16 are shown in Fig. 8.

Material	$\max(\Delta\sigma_n)$	$\max(\Delta\sigma_{n,eff})$	$\min(\Delta\tau)$	Critical Plane
AISI 1034	20°	4°	19°	-31°
35NCD16	8°	4°	4°	-40°

Table 4: Results for crack initiation orientation.

Note that Fig. 8b and Tab. 4 reinforce the previous result that in this kind of load conditions the critical plane model lead to severe mistakes in the estimation of the initial crack angle. Considering  $\max(\Delta\sigma_n)$  a better response was obtained again, however, as explained before this variable lead to the violation of a basic principle of the fracture mechanics (cracks should not propagate when they are closed). Therefore, considering this aspect and the results obtained for both materials the criterion chosen to predict the first orientation of the crack propagation hereinafter will be the critical direction method combined with the minimum shear stress range.

## RESULTS FOR CRACK PROPAGATION

### Contact modelling and stress intensity factor achievement

For each plane fretting test configuration described in Tab. 2, a 2D-plain strain FEM was implemented in Abaqus. The models were composed from a cylinder submitted to normal and tangential loads pressed against a fixed plane, Fig. 9a. Contact interactions were described by Lagrange multiplier with a friction coefficient  $f$ . The crack tip zone was meshed in a round domain of 5  $\mu\text{m}$  radius with a mesh of approximately 0.5  $\mu\text{m}$  quadrilateral linear elements, Fig. 9b. The mesh in the contact zone was refined down to 20  $\mu\text{m}$  by triangular linear elements. The coefficient of friction between crack faces was assumed to be the same one that occur in the slip zones for the cylindrical contacts in the fretting tests. The stress intensity factor was obtained by a contour integrals Abaqus routine.

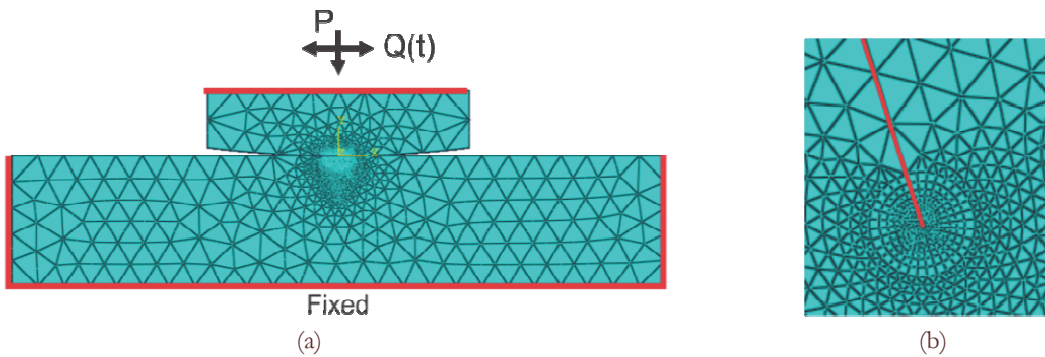
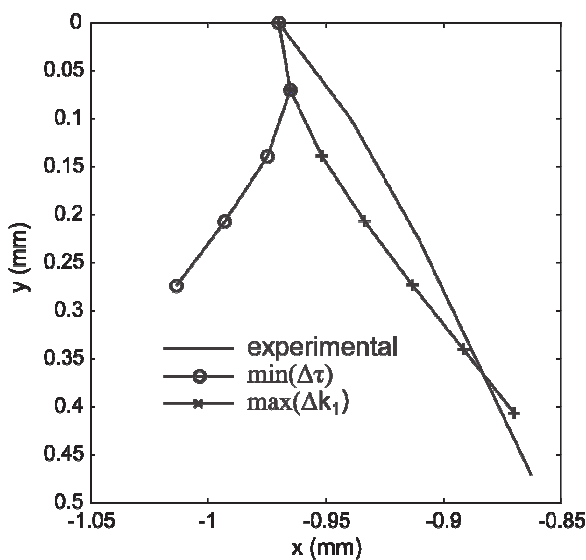


Figure 9: FEM modelling (a) contact configuration; (b) illustration of the mesh refinement at the crack tip.

### Crack propagation modelling

As described previously the crack propagation path was assessed only for 35NCD16 due to the fact that only in this case we have the experimental crack path profile for a long crack. Therefore, from the initial angle of propagation estimated, simulations were carried out with increments of crack length,  $\Delta b$ , where in each step the stress intensity factors mode I and II along a period were extracted as well as the stress field near to the crack tip. The direction of crack propagation in each step was defined applying two different methodologies, namely, the  $\max(\Delta k_1(\theta))$  in an infinitesimally kinked crack emerging from the original one or searching the material plane where the minimum shear stress range at the crack tip is reached[7],  $\min(\Delta\tau)$ . The first step to apply this model is to define an initial crack (length and direction) in the specimen. In this setting, it was assumed that this crack had an initial length  $\Delta b=70\mu\text{m}$  and its initiation angle was given by the critical direction method in terms of  $\min(\Delta\tau)$ , i.e., 4°. Fig. 10 shows the crack path simulation considering both criteria. As shown in [7] the increment size does not exert significant influence in global aspects, hence, a relatively high increment was considered to simplify the analysis.

Figure 10: Results for crack path simulation,  $\Delta b=70\mu\text{m}$ .

Note that although the initial estimate of crack initiation path was  $4^\circ$  while the actual path was  $17^\circ$ , the direction of crack propagation obtained via  $\max(\Delta k_1)$  tends to the location of the real crack as it becomes larger. However, the  $\min(\Delta\tau)$  criterion leads to a complete different path that has no correlation at all with the experimental result.

## CONCLUSIONS

**S**ome methodologies to predict the direction of crack initiation and further propagation under fretting conditions were assessed, where available experimental data were used to evaluate the accuracy of the methodologies. Two methods based on critical distances to estimate the crack initiation planes were studied. The critical direction method, provided better results than the critical plane model, which was not able to produce any reasonable estimates of crack initiation direction. In order to predict the crack propagation path two distinct methodologies were applied, one based on the maximum SIF range mode I in an infinitesimal kinked crack with origin in the pre-existent crack and another based on the stress field near to the crack tip. The criteria based on stress field,  $\min(\Delta\tau)$ , led to inconsistent predictions, whereas the criteria based on SIF, provided good agreement with the experimental response, even from a not so good choice for the direction of crack initiation. Further work mainly for earlier stages of crack birth need to be conducted in order to establish more accurate estimates of crack path in fretting conditions.

## REFERENCES

- [1] Araújo, J.A., Nowell, D., Analysis of pad size effects in fretting fatigue using short crack arrest methodologies, *Int J Fatigue*, 21 (1999) 847-856.
- [2] Dubourg, M.C., Lamacq, V., Stage II crack propagation direction determination under fretting fatigue loading: a new approach in accordance with experimental observations. In: Hoepplner DW, et al., editors. *Fretting fatigue: current technology and practices*, ASTM STP 1367, West Conshohocken; (2000) 436-450.
- [3] Susmel, L., Taylor, D., Non-propagating cracks and high-cycle fatigue failures in sharply notched specimens under in phase Mode I and II loading, *Eng F Analysis*, 14 (2007) 861-876.
- [4] Taylor, D., Geometrical effects in fatigue: a unifying theoretical model, *Int J Fatigue*, 21 (1999) 413-420.
- [5] Susmel, L., Taylor, D., Can the conventional high-Cycle multiaxial fatigue criteria be re-interpreted in terms of the theory of critical distances? *SDHM*, 2 (2006) 91-180.
- [6] Taylor, D., *The Theory of Critical Distances*. Oxford: Elsevier. 1st edition, (2007).



- 
- [7] Giner, E., Sabsabi, M., Ródeans, J., Fuenmayor, J.F., Direction of crack propagation in a complete contact fretting-fatigue, *Int J Fatigue*, 58 (2014) 172-180.
  - [8] Erdogan, F., Sih, G.C., On the crack extension in plates under plane loading transverse shear, *J Basic Eng*, 85 (1963) 519-27.
  - [9] Sih, G.C., Strain-energy-density factor applied to mixed mode crack problems, *Int J Fract*, 10(3) (1972) 305-321.
  - [10] Palaniswamy, K., Knauss, W.G., Propagation of a crack under general, in-plane tension, *In J Fract*, 8(1) (1972) 114-117.
  - [11] Ribeaucourt, R., Baietto-Dubourg, M.C., Gravouil, A., A new fatigue frictional contact crack propagation model with the coupled X-FEM/LATIN method, *Comput Methods Appl Mech Eng*, 196 (2007) 3230-3247.
  - [12] Hourlier, F., Pineau, A., Fatigue crack path behavior under complex mode loading. In: Francois D, editors. *Advances in fracture research*, Proc 5th Int Conference on Fracture. Pergamon, Oxford; (1981) 1841-1849.
  - [13] Amestoy, M., Bui, H.-D., Dang, Van K., Déviation infinités d'une fissure dans une direction arbitraire. *CR Acad Sci Paris*, 289B (1979) 99-102.
  - [14] Fouvy, S., Nowell, D., Nubiak, K., Hills, D.A., Prediction of fretting crack propagation based on a short crack methodology, *Engineering Fracture Mechanics*, 75 (2008) 1605-1622.
  - [15] Baietto, M.C., Pierres, E., Gravouil, A., Berholt, B., Fouvy, S., Trolle, B., Fretting fatigue crack growth simulation based on a combined experimental and XFEM strategy, *Int J Fatigue*, 47 (2013) 31-43.
  - [16] Proudhon, H., Fouvy, S., Determination and prediction of the fretting crack initiation: introduction of the (P,Q,N) representation of a variation process volume, *Int J Fatigue*, 28 (2005) 707-713.
  - [17] Susmel, L., Atzori, B., Meneghetti, G., Material fatigue properties for assessing mechanical components weakened by notches and defects, *Fatigue Fract Engng Mater Struct*, 28 (2005) 1-15.